PERFORMANCE AND COST EFFECTS OF NANOREFRIGERANTS WITHIN A LOW-TEMPERATURE ORC FOR WASTE HEAT RECOVERY

George Kosmadakis *, Panagiotis Neofytou

Laboratory of Thermal Hydraulics & Multiphase Flow
National Center for Scientific Research "Demokritos"
Patriarchou Grigoriou & Neapoleos 27, 15341, Agia Paraskevi, Greece

* Corresponding Author: gkosmad@ipta.demokritos.gr

ABSTRACT

The mixing of nanoparticles (NPs) with refrigerants introduces some favourable effects, with the main being the heat transfer enhancement during boiling and condensation. However, the resulting effective viscosity increases for higher NP loading, resulting to a larger pressure drop. Various nanorefrigerants have been examined in refrigeration and heat pump units, demonstrating the heat transfer coefficient increase. The present work provides some further insights of nanorefrigerants in an ORC supplied by a low-temperature heat source of 100 ^{o}C, employing R245fa and R1234ze(Z) as the base fluids. For this purpose, an existing thermodynamic model is extended to account for these particles, introducing their effect in the energy balance, and the heat transfer and pressure drop correlations.

Two NP materials with different thermophysical properties are considered, already used in many refrigeration cases, namely Al_2O_3 and Cu. The numerical model has been applied to simulate the ORC with a variable NP mass fraction (from 0 up to 10% wt.), with the aim to identify the performance improvement. Focus is given on the heat transfer coefficients in the evaporator and the condenser, as well as the pressure drop in the different parts of the cycle.

The results show that the thermal efficiency slightly increases for higher NP mass fraction and especially with the use of Al_2O_3. This is mostly attributed to the expansion process, in which the NPs act as internal heat sources to the vapour organic fluid during this process. The effect of the NPs on the heat transfer process in the two heat exchangers is minor, due to their low volume fraction in the vapour phase, resulting to small changes in the thermal conductivity. The increase in the pressure drop is minor even if the effective viscosity increases for higher NP mass fraction.

Finally, a preliminary cost analysis of the nanorefrigerants in an ORC has been conducted, showing that their use results to a payback period of 12.8 years with Al_2O_3. The sensitivity analysis revealed that this period can be reduced to half, assuming that they can sustain a long-term operation under cycling conditions.

1. INTRODUCTION

There is a large interest in using nanoparticles (NPs) as additives to the refrigerant of a vapour compression unit (Nair et al., 2016), resulting to the so-called nanorefrigerant. The latter possesses several interesting features, the main of which is the increase of the heat transfer coefficient (HTC) (Celen et al., 2014), as the result of the superior thermal conductivity of the nanorefrigerant compared to the base fluid. The augmentation of heat transfer takes place at both liquid and vapour phases and the two-phase region (Sun and Yang, 2014). However, the use of NPs induces a higher effective viscosity compared to the base fluid, increasing the pressure drop and the compressor power in vapour compression cycles (Alawi et al., 2015). There are many relevant experimental studies (Azmi et al., 2017) supporting this performance increase with different pairs of base fluids and NPs (Sanukrishna et al., 2018), but few theoretical works such as a very recent study (Kosmadakis and Neofytou, 2019), include all related mechanisms towards a detailed thermodynamic analysis of the heat pump cycle.

Similar studies for the ORC technology are limited, although the same advantages of the nanofluid exist. The heat transfer augmentation from the heat source and to the heat sink can lead to either lower surface of the heat exchangers (reduction of the capital cost) or lower pinch point temperature difference (increase of the thermal efficiency). The use of nanofluids with silver nanoparticles have been examined in a solar ORC (Saadatfar et al., 2014a), calculating a superior exergy efficiency. Similar conclusions have been reached in another work by the same group (Saadatfar et al., 2014b). In a more recent work (Mondejar et al., 2017), the effect of different nanoparticles on the heat exchanger surface and pump power consumption was studied, resulting to a promising outcome for this unexplored field.

Although there are plenty of works focusing on the heat transfer and pressure drop effects of nanorefrigerants, including the operating conditions of ORC units (Jiang et al., 2018), the complete analysis of the ORC power cycle is not yet examined. The main aim of this work is to effectively cover this gap, by conducting a detailed numerical analysis of the ORC operation using nanorefrigerants with a variable NP mass fraction, and investigating their effect on the thermal efficiency. The most recent and reliable heat transfer and pressure drop correlations are considered. Focus is given on the thermodynamic expressions for the energy and mass balance at the cycle locations, by introducing the effect of NPs. The cost-effectiveness of this solution is also examined, in order to identify the additional cost due to NPs and related cost figures.

2. NUMERICAL MODEL

A simulation model is developed in ESS software (Klein, 2018), which has built-in libraries of the properties of refrigerants and materials. This model includes the effect of NPs on the fluid’s properties, adjusting the heat transfer and pressure drop (Kosmadakis and Neofytou, 2019). A low-temperature heat source of about 100 kW at 100 ^oC is considered.

2.1 Description of the numerical model

The model is based on the energy balance of each main component. The heat transfer at the evaporator and condenser is calculated by the expressions of Equations (1a) and (1b) respectively, equal to the sum of the heat flow of the base fluid and the particles.

$$Q_{ev} = \dot{m}_R\left(h_{ev,R,out} - h_{ev,R,in}\right) + \dot{m}_{NP}\left(h_{ev,NP,out} - h_{ev,NP,in}\right) \tag{1a}$$

$$Q_{cd} = \dot{m}_R\left(h_{cd,R,in} - h_{cd,R,out}\right) + \dot{m}_{NP}\left(h_{cd,NP,in} - h_{cd,NP,out}\right) \tag{1b}$$

where $\dot{m}_R$ is the refrigerant mass flow rate, $\dot{m}_{NP}$ is the NP mass flow rate, $h_{ev,R,out/in}$ is the refrigerant enthalpy at the evaporator outlet and inlet respectively, $h_{ev,NP,out/in}$ is the NPs enthalpy at the evaporator outlet and inlet respectively, $h_{cd,R,out/in}$ is the refrigerant enthalpy at the condenser outlet and inlet respectively, and $h_{cd,NP,out/in}$ is the NPs enthalpy at the condenser outlet and inlet respectively.

The pumping process is simulated based on a constant isentropic efficiency equal to 60%, with the NPs having a negligible effect on this process except from the increased pressure drop, as shown later.

The expansion process considers the heating effect of the NPs, given by Equation (2) (Kosmadakis and Neofytou, 2019), which slightly increases the power production (the subscript *Ex* denotes the expander). This process resembles the oil-flooded expansion, in which the hot oil assists in maintaining a higher temperature and approaching isothermal process. The main difference here is that these solid particles are incompressible and do not affect the volumetric expansion of the working fluid (they do not participate in the expansion process). A constant isentropic efficiency ($n_{Ex,is}$) equal to 70% is used to model the power production process of the superheated vapour. The nanorefrigerant at the end of the expansion has a temperature higher by few degrees compared to the case of base fluid only. However, this approach entails uncertainties and should therefore be validated through experiments.

$$W_{Ex} = \dot{m}_R\left(h_{Ex,R,in} - h_{Ex,R,out,is}\right)n_{Ex,is} + \dot{m}_{NP}\left(h_{Ex,NP,in} - h_{Ex,NP,out}\right) \tag{2}$$

where $h_{Ex,R,out,is}$ is the enthalpy for isentropic expansion, without considering the heating effect of NPs.

2.2 Heat transfer and pressure drop correlations

The heat transfer analysis is based on the LMTD method, dividing the heat exchanger (HEX) into liquid, two-phase, and vapour zones (Kosmadakis and Neofytou, 2019). The heat transfer coefficients and pressure drop are calculated from the proposed correlations of Table 1. The thermophysical properties of the nanorefrigerant are included in these expressions, provided in the next section.

Table 1: Heat transfer coefficients and pressure drop correlations

	Heat transfer correlation	**Pressure drop correlation**
Single phase (liquid or vapour)	Martin, 1996	
Boiling	Amalfi et al., 2016	
Condensation	Longo et al., 2015	Kuo et al., 2005
Piping	-	Darcy-Weisbach (Romeo et al., 2002)

2.3 Thermophysical properties of nanorefrigerants

The NP mass fraction (ω) is in the range of 0-10%, with the volume fraction (φ) given by Equation (3). The volume fraction changes at the different parts of the cycle and is required, since the thermophysical properties are expressed as functions of this fraction, as shown in Table 2.

$$\varphi = \frac{\omega\, \rho_R}{\omega\, \rho_R + (1-\omega)\rho_{NP}} \tag{3}$$

where ρ_R is the refrigerant density and ρ_{NP} is the NP density.

Table 2: Thermophysical properties of nanorefrigerants

Nanorefrigerant property	**Correlation**	**Reference**
Density (ρ_{NR})	$\rho_{NR} = \varphi\, \rho_{NP} + (1-\varphi)\rho_R$	Alawi et al., 2015
Specific heat capacity ($c_{p,NR}$)	$c_{p,NR} = \frac{\varphi\, \rho_{NP}\, c_{p,NP} + (1-\varphi)\rho_R\, c_{p,R}}{\rho_{NR}}$	Alawi et al., 2015
Effective viscosity (μ_{NR})	$\frac{\mu_{NR}}{\mu_R} = 1 + 2.5\varphi + 6.5\varphi^2$	Batchelor, 1977
Thermal conductivity (k_{NR})	$\frac{k_{NR}}{k_R} = \frac{k_{NP} + (n-1)k_R - (n-1)\varphi(k_R - k_{NP})}{k_{NP} + (n-1)k_R + \varphi(k_R - k_{NP})}$	Hamilton and Crosser, 1962

2.4 Cost parameters

The cost analysis provides an indication of the cost-effectiveness of the ORC with nanorefrigerants and is based on the additional cost due to the NPs, related to the initial cost and the running costs, without considering any ORC efficiency degradation over time. The cost depends on the NP cost, using commercial prices from Sigma Aldrich, and the required quantities based on the refrigerant quantity calculated from the volume of the HEXs, piping and receiver. The preparation cost of the nanorefrigerant is assumed 50% of the NP cost, which has a high uncertainty and subjected to a sensitivity analysis. For estimating the running costs, the whole working fluid (including the NPs) is assumed to be replaced every 10 years. The result is the calculation of the discounted payback period (PBP), using a discount rate (r) of 3%, given by Equation (4) (Bhandari, 2009).

$$PBP = \frac{ln\left(\frac{1}{1-\frac{C_{in} r}{E_s - C_r}}\right)}{ln(1+r)} \tag{4}$$

where C_{in} is the additional initial cost of the NPs and nanorefrigerant preparation, C_r is the additional annual running cost, and E_s is the annual electricity value (in €/year).

3. OPERATING AND DESIGN CONDITIONS AND NANOREFRIGERANTS

3.1 Operating and design conditions

The heat source of the ORC is hot water at 100 °C with a mass flow rate of 3 kg/s (heat input about 100 kW). The condenser heat is rejected to the cold water at 20 °C with the same mass flow rate. Both evaporator and condenser are plate heat exchangers with a pinch point temperature difference of 5 K (with a superheating and subcooling imposed to 5 K). The swept volume of the expander is 165 cm^3/rev, operating at a rotational speed of 3000 rpm and with a constant filling factor of 1.2, for calculating the refrigerant mass flow rate, according to the inlet volume flow rate.

3.2 Nanorefrigerants

The screening of the refrigerants is based on the fluids commonly used in ORC for a heat source temperature of 100 °C. A common HFC refrigerant in ORC units is R245fa, examined in the current work. However, R245fa has a high GWP of 1030 and will be phased-out in the next years. Therefore, its HFO replacement, R1234ze(Z), with a low GWP below 10 is also included in the calculations. The selection of NPs is based on the ones that have demonstrated a significant heat transfer increase in the literature. Cu and Al_2O_3 are selected (Cheng and Liu, 2013) with the main properties given in Table 3.

Table 3: Properties of the selected NPs at a temperature of 25 °C

Nanoparticle	Thermal conductivity (W/m-K)	Density (kg/m^3)	Specific heat capacity (kJ/kg-K)
Cu	396.5	8958	0.389
Al_2O_3	38.7	3970	0.765

4. RESULTS AND DISCUSSION

4.1 Effect of NPs on the ORC performance

The simulations are conducted for a variable NP mass fraction in the range of 0-10% with the two refrigerants and the two NPs. For the operating and design conditions presented in the previous section, the resulting thermal efficiency and power production as a function of the NP mass fraction is shown in Fig. 1 for all organic fluids and NPs.

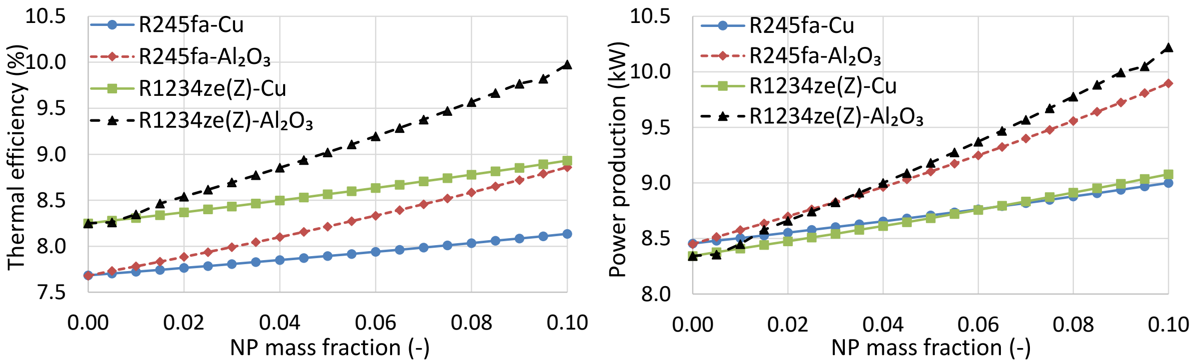

Figure 1: ORC thermal efficiency (left) and power production (right) as a function of the NPs mass fraction

The efficiency increases for higher NP mass fraction for both working fluids with similar trend. The largest increase is observed with Al_2O_3 by up to 20%, due to its higher specific heat capacity than Cu (see Table 3), approaching even more the isentropic expansion, according to Equation (2). For this set of conditions, the ORC with R1234ze(Z) shows a slight higher efficiency. But the power production is similar, since the heat input of R1234ze(Z) is 8 kW lower (96 kW instead of 104 kW with R245fa).

4.2 Effect of NPs on the heat transfer and pressure drop processes

The enhancement of heat transfer by the nanorefrigerant is clear in Fig. 2, showing the HTC during boiling and condensation for all working fluids as a function of the NP mass fraction.

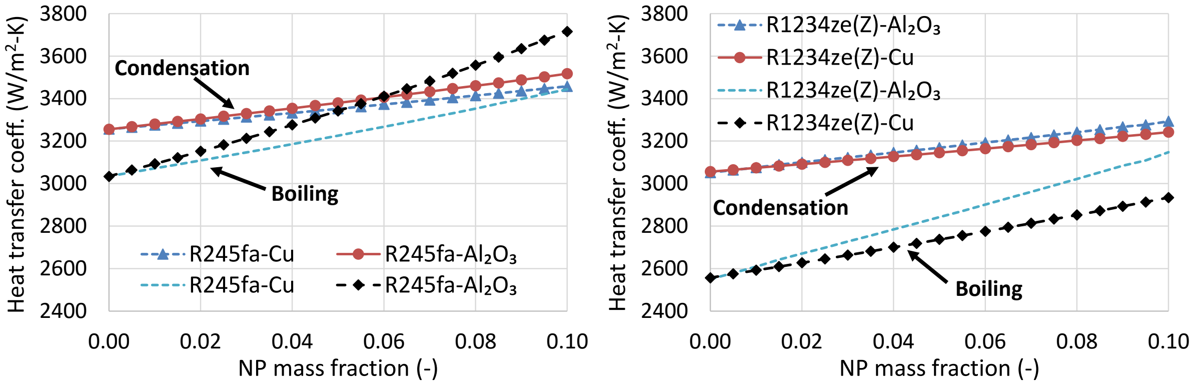

Figure 2: Heat transfer coefficients for boiling and condensation as a function of the NPs mass fraction

In general, the HTCs with R245fa are higher than with R1234ze(Z), especially during boiling. Both NPs introduce a similar increase of the HTC during condensation, while during boiling the use of Al_2O_3 brings an even higher increase, due to its higher volume fraction, increasing to a larger extent the thermal conductivity and effective viscosity. The HTC increase is also attributed to the higher density and mass flux (up to 3-4%) of the nanorefrigerant compared to the base fluid.

The total pressure drop is divided into the drop in the condenser, the evaporator, and the piping. The relative pressure drop compared to the pressure drop without NPs with R245fa and the two NPs is shown in Fig. 3. Similar trend is also applied with R1234ze(Z), and thus not shown here. The total pressure drop is also presented in Fig. 3 (bottom) as a function of the NP mass fraction.

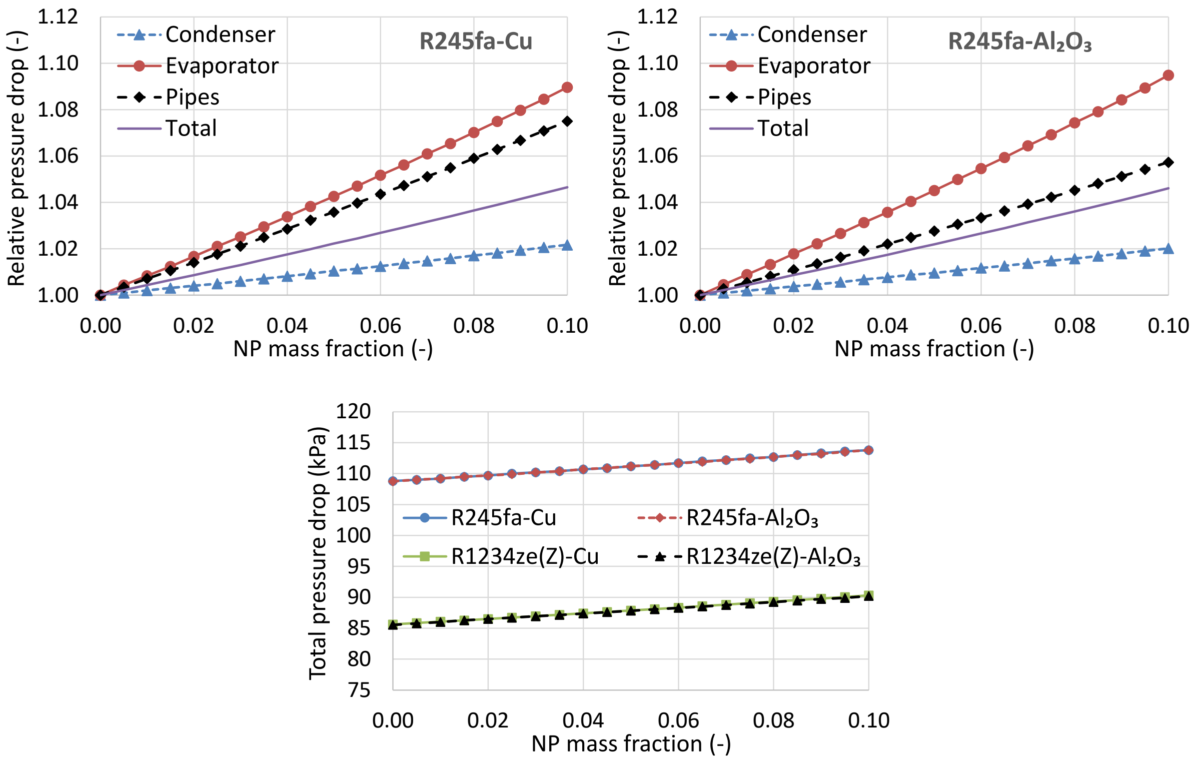

Figure 3: Top: Relative pressure drop in the condenser, evaporator, piping and the total one with Cu (left) and Al_2O_3 (right) as a function of NPs mass fraction; Bottom: Total pressure drop as a function of NPs mass fraction

The highest effect of NPs on the pressure drop is observed in the piping. However, this drop in absolute numbers is low compared to the ones in the HEXs, with the pressure drop in the evaporator being 3-4 times higher than in the condenser. The total pressure drop increases by up to 4.5%, with the pump consuming more power to compensate for this loss (up to 2%, corresponding to 5 kPa in absolute values). This pump power increase is negligible, as also concluded by Mondejar et al. (2017).

Except from the effective viscosity ratio, which is similar for both NPs (slightly higher for Al_2O_3), there are other properties that affect the pressure drop, such as the density. Cu is about two times more dense than Al_2O_3, increasing the nanorefrigerant density, and the relative pressure drop. The pressure drop in absolute values is 30% higher with R245fa as with R1234ze(Z) due to the higher R245fa mass flow rate, which increases accordingly the mass flux and the pressure drop (Zhang et al., 2017).

4.3 Cost analysis

Based on the previous results, the discounted payback period is calculated, shown in Fig. 5 for three NP mass fractions as a function of the capacity factor (equivalent to operational hours per year). The results are shown only with Al_2O_3, since with Cu this period is always higher than 60 years (with both refrigerants), much higher than the ORC lifetime.

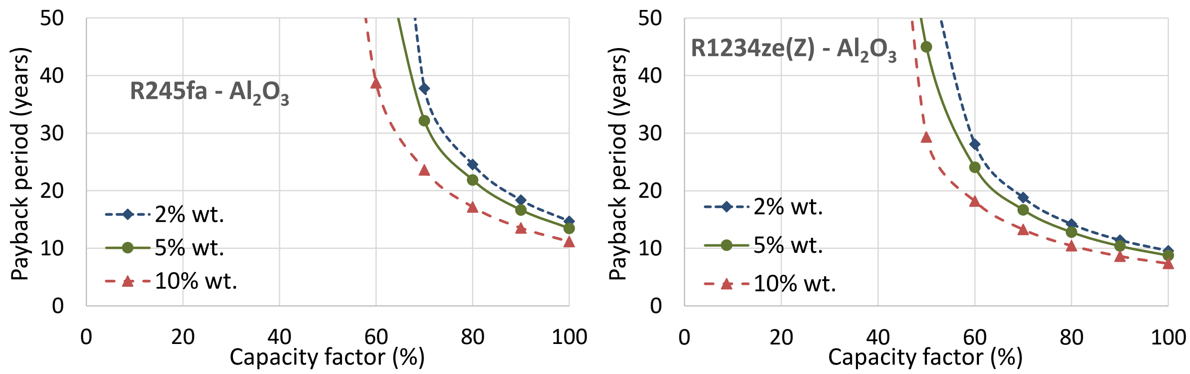

Figure 5: Payback period of the ORC with nanorefrigerant for different Al_2O_3 mass fraction

The PBP is shorter with R1234ze(Z), as a result of its superior performance. Moreover, the use of Al_2O_3 makes it possible to reach a PBP of slightly less than 10 years for the highest NP mass fraction and a 100% capacity factor. In any case, the NP mass fraction and capacity factor have the decisive role on the resulting PBP, and mostly the latter parameter. High capacity factors are needed, more than 80%, in order to utilize this configuration as much as possible, and make it possible to achieve a short payback period.

4.4 Sensitivity analysis of cost effectiveness

A sensitivity analysis is included in this work, due to the large uncertainty of some parameters given in Table 4 that includes their minimum and maximum values, except from the ones used above (standard values).

Table 4: Parameters of the sensitivity analysis and their range

Parameter	**Minimum**	**Standard**	**Maximum**
Refrigerant charging (kg)	20	30	40
Al_2O_3 cost (€/kg)	900	1800	3600
Cost increase of nanorefrigerant preparation (%)	25	50	100
Electricity price (€/kWh)	0.05	0.10	0.15
Discount rate (%)	2	3	5

The case of R1234ze(Z) is selected due to its superior economic performance over R245fa, as revealed in Fig. 5, and its low GWP value. Al_2O_3 is selected with a reasonable mass fraction of 5%. The capacity factor is 80%, corresponding to almost continuous operation, such as for waste heat recovery, but not solar thermal energy. The discounted PBP of this analysis is shown in Fig. 6 with the standard case having a PBP of 12.8 years.

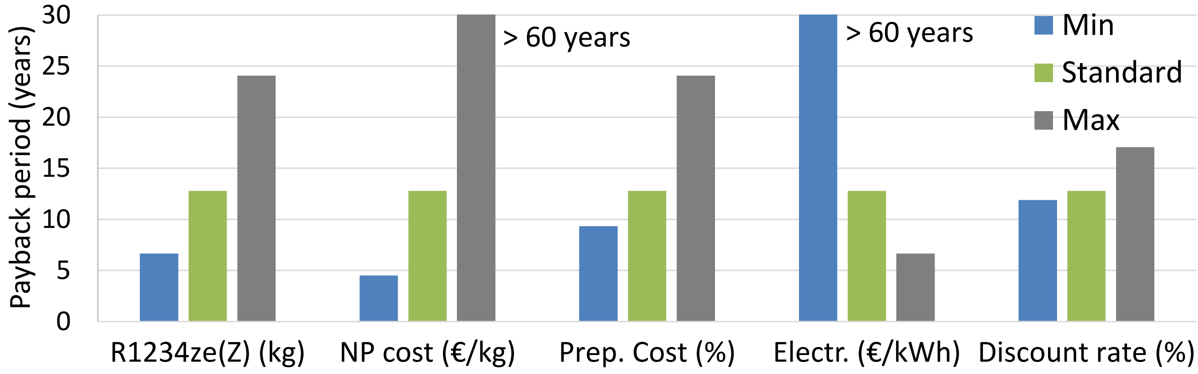

Figure 6: Sensitivity analysis of the payback period

By reducing the refrigerant charge, the NP amount is reduced accordingly, which is highly beneficial for the nanorefrigerant's cost-effectiveness. A similar effect is introduced with the NP cost reduction, reaching a PBP of 4.5 years. The nanorefrigerant's preparation cost has a very large uncertainty, since it is unknown how this could evolve in industrial scale, having although a moderate effect on the PBP. Moreover, the electricity price is directly related to the annual income, with the PBP increasing to over 60 years for low prices. Finally, the discount rate has a small effect on PBP. In most of the cases, the PBP remains in the range of 4.5-24 years. However, there are further steps to be conducted before a commercial ORC with nanorefrigerants becomes available, and this progress is highly related to the materials stability and long-term operation under continuous cycling conditions, as well as a more detailed investigation of the nanorefrigerant cost.

5. CONCLUSIONS

A detailed numerical model including the pressure drop is developed and applied for the simulation of an ORC with the use of two NPs of variable mass fraction and two refrigerants. The effect of the NPs has been introduced in the energy balance of the thermodynamic analysis and on the correlations of heat transfer and pressure drop.

The results initially concern the ORC performance, showing its increase by up to 20% for higher NP mass fraction. The use of Al_2O_3 over Cu is preferred in terms of performance, with the main driver the higher power production in the expander. The heat transfer and pressure drop were also examined, revealing that the effect of both NPs is rather small. The overall outcome is that the Al_2O_3 introduces a higher performance and enhanced HTCs, making it possible to decrease the HEX surface area.

Finally, the preliminary cost analysis indicated that the use of a nanorefrigerant could be a sustainable solution for the ORC technology, with a standard PBP of 12.8 years for Al_2O_3 that can be reduced to even 4.5 years in favourable conditions. However, this cost analysis should be enriched with a more reliable expression/correlation of the nanorefrigerant's preparation cost. Except from that, the verification of the nanorefrigerant's stability for a long-term operation is crucial, which is an unexplored activity.

REFERENCES

Alawi, O.A., Sidik, N.A.C., Kherbeet, A.S., 2015. Nanorefrigerant effects in heat transfer performance and energy consumption reduction: A review. International Communications in Heat and Mass Transfer 69, 76–83.

Amalfi, R.L., Vakili-Farahani, F., Thome, J.R., 2016. Flow boiling and frictional pressure gradients in plate heat exchangers. Part 2: Comparison of literature methods to database and new prediction methods. International Journal of Refrigeration 61, 185–203.

Azmi, W.H., Sharif, M.Z., Yusof, T.M., Mamat, R., Redhwan, A.A.M., 2017. Potential of nanorefrigerant and nanolubricant on energy saving in refrigeration system–A review. Renewable and Sustainable Energy Reviews 69, 415–428.

Batchelor, G.K., 1977. The effect of Brownian motion on the bulk stress in a suspension of spherical particles. Journal of fluid mechanics 83, 97–117.

Bhandari, S.B., 2009. Discounted payback period-some extensions. J. Bus. Behav. Sci 21, 28–38.

Celen, A., Çebi, A., Aktas, M., Mahian, O., Dalkilic, A.S., Wongwises, S., 2014. A review of nanorefrigerants: flow characteristics and applications. International Journal of Refrigeration 44, 125–140.

Cheng, L., Liu, L., 2013. Boiling and two-phase flow phenomena of refrigerant-based nanofluids: fundamentals, applications and challenges. International Journal of Refrigeration 36, 421–446.

Hamilton, R.L., Crosser, O.K., 1962. Thermal conductivity of heterogeneous two-component systems. Industrial & Engineering chemistry fundamentals 1, 187–191.

Jiang, F., Zhu, J., Xin, G., 2018. Experimental investigation on Al2O3-R123 nanorefrigerant heat transfer performances in evaporator based on organic Rankine cycle. International Journal of Heat and Mass Transfer 127, 145–153.

Klein, S.A., 2018. Engineering Equation Solver EES Academic Professional.

Kosmadakis, G., Neofytou, P., 2019. Investigating the effect of nanorefrigerants on a heat pump performance and cost-effectiveness. Thermal Science and Engineering Progress, 100371.

Kuo, W.S., Lie, Y.M., Hsieh, Y.Y., Lin, T.F., 2005. Condensation heat transfer and pressure drop of refrigerant R-410A flow in a vertical plate heat exchanger. International Journal of Heat and Mass Transfer 48, 5205–5220.

Longo, G.A., Righetti, G., Zilio, C., 2015. A new computational procedure for refrigerant condensation inside herringbone-type Brazed Plate Heat Exchangers. International Journal of Heat and Mass Transfer 82, 530–536.

Martin, H., 1996. A theoretical approach to predict the performance of chevron-type plate heat exchangers. Chemical Engineering and Processing: Process Intensification 35, 301–310.

Mondejar, M.E., Andreasen, J.G., Regidor, M., Riva, S., Kontogeorgis, G., Persico, G., Haglind, F., 2017. Prospects of the use of nanofluids as working fluids for organic Rankine cycle power systems. Energy Procedia 129, 160–167.

Nair, V., Tailor, P.R., Parekh, A.D., 2016. Nanorefrigerants: A comprehensive review on its past, present and future. International Journal of Refrigeration 67, 290–307.

Romeo, E., Royo, C., Monzón, A., 2002. Improved explicit equations for estimation of the friction factor in rough and smooth pipes. Chemical engineering journal 86, 369–374.

Saadatfar, B., Fakhrai, R., Fransson, T., 2014a. Exergo-environmental analysis of nano fluid ORC low-grade waste heat recovery for hybrid trigeneration system. Energy Procedia 61, 1879–1882.

Saadatfar, B., Fakhrai, R., Fransson, T., 2014b. Conceptual modeling of nano fluid ORC for solar thermal polygeneration. Energy Procedia 57, 2696–2705.

Sanukrishna, S., Murukan, M., Jose, P.M., 2018. An overview of experimental studies on nanorefrigerants: Recent research, development and applications. International Journal of Refrigeration 88, 552–577.

Sun, B., Yang, D., 2014. Flow boiling heat transfer characteristics of nano-refrigerants in a horizontal tube. International Journal of Refrigeration 38, 206–214.

Zhang, J., Desideri, A., Kærn, M.R., Ommen, T.S., Wronski, J., Haglind, F., 2017. Flow boiling heat transfer and pressure drop characteristics of R134a, R1234yf and R1234ze in a plate heat exchanger for organic Rankine cycle units. International Journal of Heat and Mass Transfer 108, 1787–1801.

ACKNOWLEDGEMENT

This work has been conducted within the framework of the Industrial Scholarships program of the National Center for Scientific Research “Demokritos”, co-funded by Stavros Niarchos Foundation.